A general method for near-infrared photoswitching in biology, demonstrated by the >700 nm photocontrol of GPCR activity in brain slices

Benedikt Baumgartner[1], Viktorija Glembockyte[2,3], Alberto J. Gonzalez-Hernandez[4], Abha Valavalkar[5], Robert Mayer[2], Lucy L. Fillbrook[6], Adrian Müller-Deku[1], Jinhua Zhang[7], Florian Steiner[2,3], Christoph Gross[2], Martin Reynders[1], Hermany Munguba[4], Anisul Arefin[4], Armin Ofial[2], Jonathon E. Beves[6], Theobald Lohmueller[7], Benjamin Dietzek-Ivanšic[5,8], Johannes Broichhagen[9], Philip Tinnefeld[2,3], Joshua Levitz[4], Oliver Thorn-Seshold[1]*

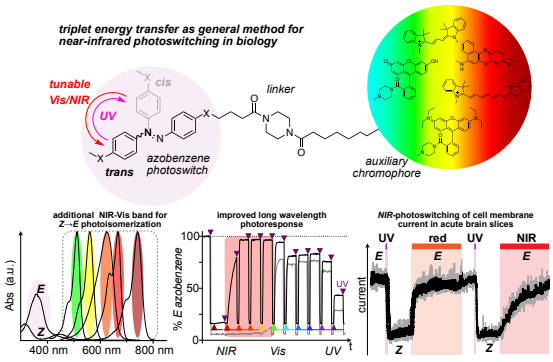

Azobenzene molecular switches are widely used to photocontrol material properties, and biological activity in cell culture, via photoisomerisation between *E* and *Z* isomers. However, because population photoswitching is incomplete, their dynamic range of property control is often small; and because they cannot be operated with red/NIR light, they are usually not applicable in deep tissue. Here, we demonstrate a general method for efficient single-photon photocontrol of azobenzenes, and of glutamate receptor activity, at >700 nm in live tissue. We use red/NIR chromophore auxiliaries to perform intramolecular energy transfer to bioactive azobenzenes, which drives fast bulk *Z*→*E* isomerisation up to even >97% completeness. The auxiliary/azobenzene dyads allow >700 nm photoswitching with photon-efficiency that can be even higher than for direct azobenzene *E*→*Z* isomerisation in the UV region; and they are biocompatible and photostable. Crucially, their performance properties are *intrinsic*, i.e. auxiliary-based intramolecular switching will perform identically at any dilution and will not be affected by biodistribution. We show that these dyads can be created straightforwardly from most azobenzene systems, with most auxiliary chromophores, without tricky molecular redesign or re-optimisation. After outlining some rules of auxiliary-based photoswitching, which can guide its broader adoption, we conclude by using dyads to make the first demonstration of single-photon NIR chemical photoswitching control over biological activity, in cell culture and intact brain tissue.

1. INTRODUCTION

Azobenzenes are the major synthetic molecular photoswitches.[1] They allow chemical effectors to be actuated with high spatial and/or temporal precision, in a range of applications from photopatterned materials[2,3] to photocontrolled biology in cell culture[4–7], in model animals[8,9], and recently in a human clinical trial[10]. In each use, an azobenzene scaffold is decorated with substituents so that its *E* and *Z* isomers affect the system differently; and samples are locally photoswitched between majority-*E* and majority-*Z* populations to locally pattern compound activity (**Figure 1a**).

Two major factors limit the utility of azobenzene photoswitches. In brief, (1) on the population level, *E*→100%*Z* or *Z*→100%*E* photoswitching is not possible, due to overlap of *E*/*Z* absorptions. *Z*→*E* switching is the more incomplete direction. Since *Z*-active reagents are usually targeted,[11] this results in high background activity during bidirectional photoswitching: giving *more-on/less-on* activity switching, not ideal on/off control. Even 'good' azobenzenes typically allow just ~5-fold functional dynamic range of photoswitching ("FDR": the ratio of the fraction of active isomer Φ at best "forward" isomerisation (Φ_F, e.g. *E*→*Z*) to that at best "backward" isomerisation (Φ_B, e.g. *Z*→*E*), i.e. FDR = Φ_F/Φ_B).[12] Most materials or biosystems need many-fold higher FDR, i.e., *Z*→*E* completeness (smaller Φ_B). The *Z*→*E* problem is worsened in practice, since *Z*→*E* switching also has much lower photon-efficiency (a metric for how much bulk isomerisation is generated per mole of photons applied; like fluorescence brightness, it is proportional to both $\varepsilon(\lambda)$ and $\varphi_{isom}(\lambda)$).[13] (2) No broadly-usable biocompatible strategy to operate azobenzenes with well-penetrating red/NIR light is known. Typical azobenzenes only respond well to light <530 nm, which is strongly scattered and absorbed in biological tissues or complex samples. Thus, most azobenzenes are limited to use in superficial, simplified, optically transparent systems (e.g. 2D cell culture or material surfaces). Together, these two limits have blocked photoswitches from many valuable applications that require high activity fold-changes deep in materials, or in tissues *in vivo*[13–16] (see **Supporting Note 1**).

Strategies to improve the completeness and photon-efficiency of *Z*→*E* photoswitching with red/NIR light, that can work in complex as well as simple systems, are highly sought after. Direct substituent tuning can rarely even achieve yellow-light photoresponse; and no generally useful, synthetically accessible, biocompatible red/NIR designs are known that do not compromise features such as *Z*-isomer stability, or bioactivity, or chemical stability. The closest approaches are green/yellow-responsive tetra-*ortho*-substitutions of Woolley, Hecht, and others,[17–21] and the strained cyclic azobenzenes of Herges[22,23]. Their switching can be more complete than with classical azobenzenes; but their visible extinction coefficients are low (ca. < 1000 $M^{-1}cm^{-1}$); far-red/NIR photoswitching is still inaccessible; and by forcing multiple substitutions around the diazene, these designs restrict the chemical and applications space available: a particular problem for photopharmacology, where these positions are often needed for target binding.

We aimed at a simple method for high-completeness as well as high-photon-efficiency *Z*→*E* photoresponse in the NIR, that can be applied practically and in complex settings. Many promising classes of photopharmaceuticals have been developed up to cell culture uses over the last two decades. We aimed to develop a general chemical approach that can retrofit them, allowing them to now be broadly applied *in vivo* in biology (thanks to an *intrinsic* method to photocontrol them in the red/NIR), without putting their target binding at risk through large molecular changes around the azobenzene. We now present methods using biocompatible *auxiliary chromophores* that absorb strongly in the green/red/NIR, then efficiently trigger selective *Z*→*E* isomerisation, to achieve this. This paper will focus on auxiliaries that inject energy for photoswitch isomerisation only by first entering a *proximity-induced triplet* state that *then* collapses to excite the azobenzene. This concept differs importantly in its performance from what can be achieved with a *typical* triplet sensitiser auxiliary such as methylene blue or palladium porphyrin, that efficiently undergo intersystem crossing (ISC) in their isolated excited state. A parallel paper[24] is reporting on auxiliary chromophores that act via photoredox, with similar benefits.

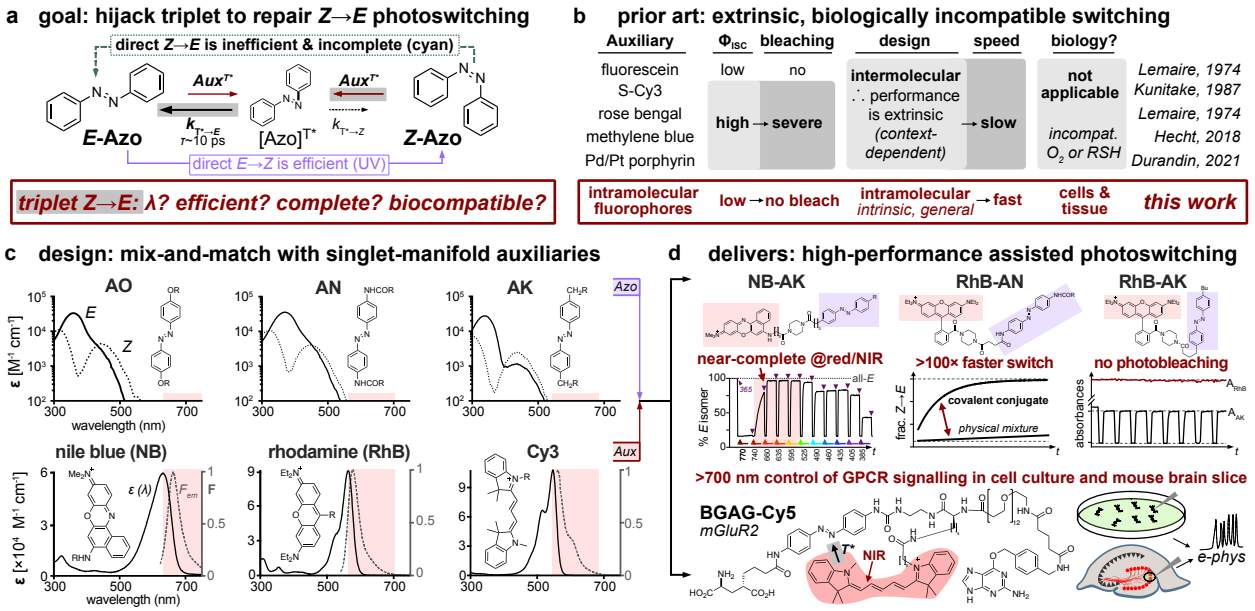

Figure 1: (**a**) Scheme of how TET-based switching may complement direct UV switching. (**b**) Intermolecular TET is known and inapplicable for biology. *This work* presents intramolecular, *proximity-induced, conditional* TET to solve the challenges of efficiency, photostability, and biocompatibility. (**c**) Spectra for typical dyad components. (**d**) Key properties of high performance conditional-TET-based photoswitching (this work).

Auxiliary chromophores that isomerise azobenzenes by single-photon processes are sparsely reported; none have been used in biology. The main known auxiliaries are triplet sensitisers (**Figure 1b**). Triplet sensitisers can perform triplet energy transfer (TET) to suitably lower-energy triplet acceptors (azobenzene: ca. 150 kJ/mol[25,26]). Azobenzene T1 states collapse to S0 after an unusually short triplet lifetime (ca. 10 ps; large spin-orbit coupling[27]), mostly giving the *E*-isomer: TET-equilibria can reach *E*:*Z* ratios ca. 0.985 : 0.015[26,28], i.e. near-complete *Z*→*E* isomerization (**Figure 1a**). There are only ten significant experimental reports in this area (**Figure 1b**; **Supporting Note 2**).[26,28–34] Though the desirability of TET-based *Z*→mostly-*E* isomerisation at wavelengths decoupled from azobenzene's own absorption is clear,[32] these systems could not be generally applied (**Supporting Note 3**). In brief, this is because they were intermolecular schemes, requiring collisional TET to the azobenzene without TET to competitive quenchers e.g. O_2 or thiols: so (i) they are unlikely to work at the high dilutions expected in biology, and (ii) they lose isomerisation efficiency by 500-fold and undergo continual photobleaching unless O_2 is excluded.[31] We thus aimed at auxiliary-azobenzene dyads for intramolecular TET to give concentration- and environment-independent *intrinsic* performance (**Figure 1c-d**; note that it has been unknown whether dyads could ever reach fully intramolecular TET, and so allow O_2-tolerance without photodamage to auxiliary, switch, biological target, or environment).

The choice of triplet sensitisers was also unclear. Prior TET schemes chose to maximise intersystem crossing yields Φ_{ISC}, so used bio-incompatible photocatalysts (redox cycling organics,[29,31] cell-impermeable heavy metal complexes[32] and dyes[30]); and by absorbing UV-blue light they reduce direct *E*→*Z* azobenzene isomerisation yields[31].

However, we had seen very photon-efficient, near-complete *Z*→*E* azobenzene isomerization upon exciting a covalently-attached Rhodamine B auxiliary.[35] The mechanism of this isomerisation was unknown, but resonant energy transfer seemed unlikely due to near-zero overlap of *Z*-azo absorbance (<530 nm) and rhodamine emission (>570 nm; **Figure S13**, **Table S2**). Since this highly photostable and biocompatible auxiliary has a vanishingly low Φ_{ISC}, we wondered if proximity to the azobenzene with its large spin-orbit coupling coefficients was driving the energy of the singlet excited auxiliary ultimately into an azobenzene triplet, that then collapsed to the observed mostly-*E* photostationary state (PSS; discussion in **Supporting Note 4**). If this were true, low-Φ_{ISC} auxiliaries might have unique power for biocompatible TET switching: (a) when the azobenzene motif contacts it, even a low-Φ_{ISC} chromophore might pump isomerisation via the triplet state with high efficiency; but (b) when the azobenzene motif is not in molecular contact (e.g. linker-extended conformation), the chromophore should stay in a biocompatible singlet manifold photocycle. (We later found a 1987 report by Targowski and coworkers, potentially showing conditional TET from rhodamine to cyclooctatetraene[36], that may support the plausibility of this idea.) This *conditional TET* might avoid the O_2-incompatibility of previous TET approaches. It would also allow using validated fluorophores, optimised for high absorption, long excited state lifetimes, and excellent biological tractability, that have known biodistribution, cell entry and localisation.

Thus, despite their small Φ_{ISC} values, we explored fluorophores such as rhodamines and cyanines as photoswitching auxiliaries. We can now report that their dyads are a generally applicable strategy for intrinsically high-performing, biocompatible, O_2-tolerant, high-photon-efficiency and near-complete *Z*→*E*-isomerisable photopharmacology tools, with red/NIR response and deep-tissue potential.

2. RESULTS

2.1 Design of conditional TET dyads

To test for conditional TET, we first excluded dyads that can perform intramolecular singlet state photoredox. For highly absorbing chromophores with low Φ_{ISC}, such dyads can be predicted from their excited state reduction potential E^{S1}_{red} (**Tables S8-S9**) and the azobenzene ground state oxidation potential (**Tables S10-S11, Figure S14**), allowing us to exclude such dyads from the present study. (In a parallel study, these values were measured, and dyads that would be predicted to undergo photoredox from these values were confirmed to undergo characteristically 100%-complete, *Z*→*E* photoredox isomerisation; see **Supporting Note 5**).[24]

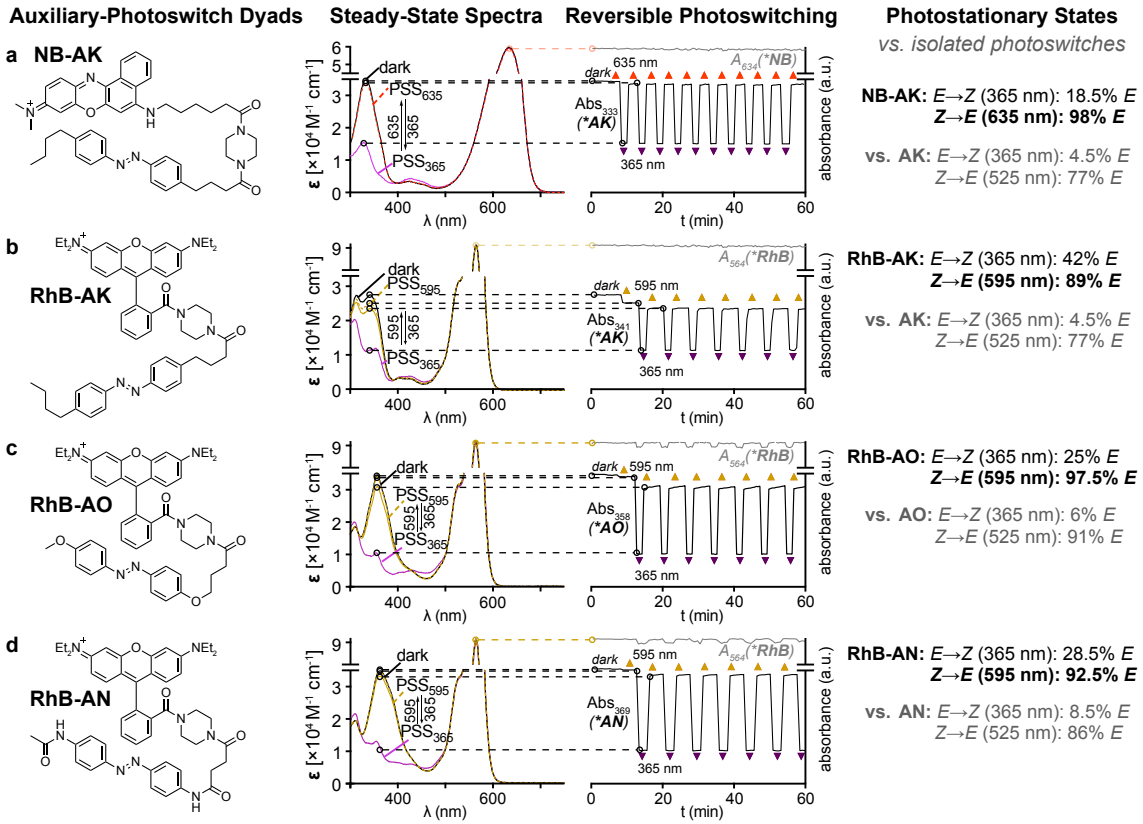

Figure 2: Azobenzene-chromophore dyads can access photostable, triplet-sensitisation-based, long-wavelength *Z*→*E* photoswitching that is nearly complete. This allows highly photostable, fast, reversible, bidirectional photoswitching with the major classes of bistable azobenzenes.

We focused on finding chromophores for "bistable" azobenzene types, i.e. those whose metastable *Z*-isomer spontaneously isomerises to the thermodynamic *E* isomer more slowly than typical experimental timescales (e.g. halflife > 12 hours; **Supporting Note 6**). These bidirectionally-photoisomerisable switch types are the ones that have been the most useful in materials and photopharmacology, and which would benefit most from better *Z*→*E* completion. This includes switches with alkyl substituents (**AK**; e.g. "photolipids"[3,37,38]), alkoxy groups at both *para* positions (**AO**; e.g. actin and tubulin cytoskeleton modulators[6,35,39–41]), and anilides at both *para* positions (**AN**; e.g. ion channel modulators[4,8,42–44]).

Electron-neutral **AK**-type azobenzenes are difficult to oxidize ($E_{1/2}(Az^{\bullet+}/Az) = E^{S0}{}_{ox}$ ~ 1.7 V vs Fc)[24], so **AK**s could be paired with nearly all chromophores we measured ($E^{S1}{}_{red}$ ~ 0.5 - 1.2 V)[24] without complications from photoredox-based processes. Electron-richer **AO** and **AN** ($E^{S0}{}_{ox}$ ~ 1 V) are compatible with e.g. xanthene and cyanine chromophore sensitisation, but were excluded from pairing with stronger photooxidants like the naphthoxazine Nile Blue (**NB**, $E^{S1}{}_{red}$ = 1.1 V)[24] (**Supporting Note 4**). The spectral and photoelectrochemical properties of the chosen azobenzenes and chromophores are summarised in **Figure 1c** and **Tables S9-S11**.

2.2 Red/NIR photoswitching in sensitisation dyads

A range of dyads with bistable **AK**, **AO** and **AN** azobenzenes connected via flexible linkers to photostable chromophores (rhodamine B **RhB**, cyanine-3 **Cy3**, Nile Blue **NB**, etc) were synthesized by standard chemistries; the dyads are denoted e.g. **RhB-AO**, **Cy3-AN**, **NB-AK** according to constitution (**Figure 2**-**3**). The dyads' photoswitching was investigated by UV/VIS spectroscopy, in dilute aqueous conditions (~10 μM), at neutral pH, under normal aerated conditions that lead to photobleaching for the known intermolecular triplet sensitiser systems[31,32]. HPLC measurements of the *E*/*Z* ratios at fixed PSSs were used to calibrate those during bulk population switching in UV-Vis: a method that is faster, cheaper, more convenient, and photochemically more appropriate, than the costly and slow in-NMR-illumination methods that are typically used[45,46] (**Supporting Information section 5**). Considering *E*→*Z* switching, the dyads were switched to a mostly-*Z* state by UV light, reaching PSS %*Z* values slightly lower than for the unconjugated azobenzenes (typically 70-85% *Z* in the dyad vs 85-95% *Z* without the chromophore), although with comparably rapid bulk photoswitching speed (**Supporting Table S3** and **Table S5**). The lower UV-PSS %*Z* is likely due to competitive absorption by the chromophores, which then promote *Z*→*E* switching (see below); but since FDR = Φ_F/Φ_B, these marginally smaller forward-switching fractions Φ_F for the dyads only slightly affect their resultant FDRs.

To analyse practical bulk photoswitching performance, we define bulk switching "rates" in this work as being proportional to the *progress of isomerisation towards PSS, per mole of photons*. Considering *Z*→*E* switching, typical unconjugated **AK, AN** and **AO** photoswitches are isomerised to 75-90% *E* by 490-525 nm light, with bulk photoswitching rates that are roughly 10-30 times smaller than for isomerisation with UV light: due to smaller extinction coefficients and more *E*/*Z*-absorbance overlap in the visible. When assays stringently use optical filters or true monochromatic light sources rather than broadband LEDs, they usually have no photoresponse above 550 nm except to high-intensity focused lasers (**Figure 3c**).

Uniquely, however, their dyads were rapidly *Z*→*E* photoisomerised by yellow/red/NIR light, with high completeness (**Figures 2-3**). Rhodamine dyads were particularly effective, with 595 nm PSSs of ≥ 97% *E* (**Figure 3a**; FDRs up to 28), and bulk *Z*→*E* yellow-light-photoswitching rates that were faster than the unconjugated azobenzenes' photoresponse to UV light (**Supporting Table S5**).

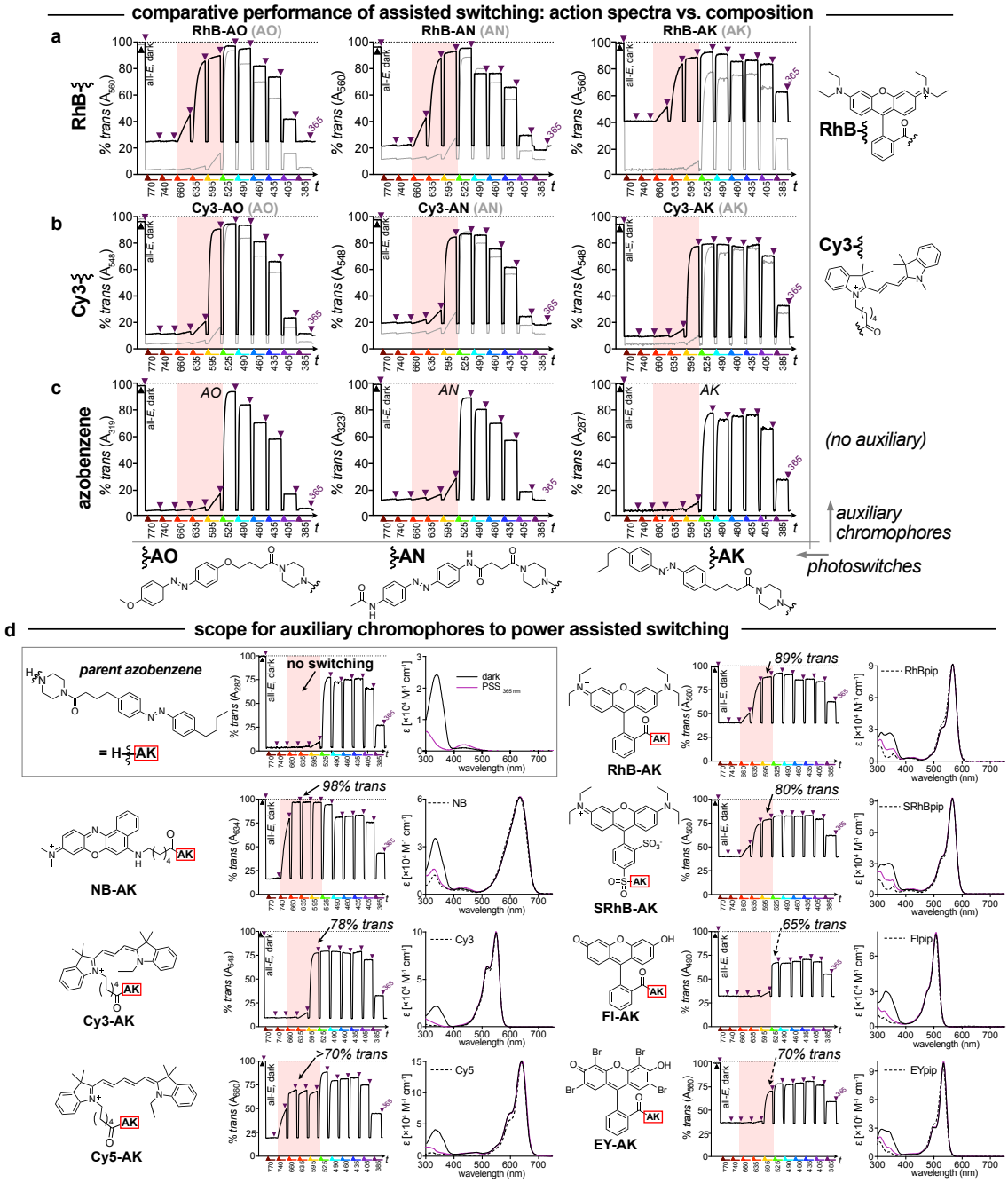

Figure 3: The spectrally-extended photoresponses of azobenzene-chromophore dyads that undergo triplet energy transfer: Action spectra (%*E* photoresponse), while phases of 365 nm (isomerises to mostly-*Z*) are alternated with phases at up to 770 nm (observation by UV-Vis, calibration to %*E* by HPLC). **(a-c)** Photoresponses of **AO**, **AN** and **AK**, and their **RhB** / **Cy3** conjugates. The longer-wavelength photoresponses of the dyads, based on absorption by the chromophore motifs (red shading), are photon-efficient and approach *E*-enriched states. **(d)** Photoresponse of **AK** and a range of its conjugates. Sensitization is a common phenomenon over a wide range of chromophore classes and absorption wavelengths. **NB-AK** shows the most-complete sensitized isomerization (98% *E*), responding up to 740 nm.

Cy 5 dyads were particularly NIR-shifted, allowing rapid *Z*→*E* photoresponses even up to ca. 750 nm (**Figure 3d**; PSS: >70% *E* with half the rate of azobenzene UV-photoswitching). For alkylazobenzene **AK** this represents a ≥250 nm bathochromic shift of *Z*→*E* switch wavelength, plus 3-fold more complete *Z*→*E* photoswitching and 20-fold faster photoresponse in the NIR dyad than with typical wavelengths used for its *Z*→*E* photoswitching (460-500 nm). Alternatively, when combined with naphthoxazine (**Figure 3d**), the **NB**-**AK** dyad reached a PSS under 635 nm light of 98% *E* and with similar bulk photoswitching rate as unconjugated **AK** under UV light (**Figure 2**; bulk photoswitching rates are determined from the "half-power" $p_{1/2}$ for half-conversion towards PSS, calibrated over a range of source intensities, and thus reflect the photon efficiency of switching: see **Figures S6-S7, Tables S3 and S5** and **Supporting Note 7**). Consistent with this sensitisation being an intrinsic, intramolecular process, 1:1 physical mixtures of the free chromophores with the azobenzenes under biologically plausible conditions (e.g. **NB** with **AK**, 10 μM each) showed no TET-assisted photoswitching: they did not respond to light >530 nm, and their response below 530 nm was almost identical to that of the free azobenzene (slightly slowed, consistent with optical shielding by the chromophores: **Figure S8**). The dyads could be reversibly

photoswitched between their PSSs by alternating phases of UV and yellow/red/NIR light over tens of cycles, with vast excesses of light applied in each phase, without or with less than 1% photodegradation observed (**Figure 2**). The photon-efficient, high-completeness, fully reversible long-wavelength photoresponse is the most important aspect of the dyads' behaviour. Further features are discussed in **Supporting Note 8**.

2.3 Spectral response profiling of sensitisation dyads

Beyond the two-colour photoswitch cycling (**Figure 2**), we also profiled the spectral photoresponses of key **RhB** and **Cy3** dyads across the NIR/Vis/nUV range (**Figure 3a-b**). All six dyads had reliable functional performance, giving more-complete and much faster *Z*→*E* photoswitching by the longer-wavelength sensitised process than by direct azobenzene photoexcitation (**Figure 3c**; see also **Table S3**). For illumination wavelengths above 525 nm, where only the **RhB**/**Cy3** chromophores absorb efficiently, their photoresponses were dominated by the mostly-complete *Z*→*E* sensitised switching process; <500 nm, their photoresponses (bulk switching speeds and PSSs reached) somewhat resemble those of the unconjugated azobenzenes, but with lower *Z*-percentages at equilibrium, consistent with residual TET-based *Z*→*E* isomerisation.

2.4 A range of chromophores can be used for sensitiser dyads

Electron-neutral azobenzenes like **AK** have hundreds of reports from materials through to chemical biology. In biological applications they are excellent lipid mimics,[47,48] and are understood to be more resistant to biothiols than electron-rich bistable switches like **AO** and **AN**. However, compared to **AO** and **AN**, they have less-complete *Z*→*E* photoswitching, and blue-shifted photoresponses, which restrict the power they could otherwise exert.[49] We had observed excellent photoswitching enhancement in **NB-AK** and **RhB-AK** dyads (**Figure 2**), so we now created a range of **AK** dyads to study how efficiently and completely different chromophores sensitise the isomerisation of these standard photoswitches (**Figure 3d**).

We found that sensitisation is a very general phenomenon (**Figure 3d**). Compared to the switch **AK**, its dyads with chromophores that absorb at longer wavelengths had longer-wavelength photoresponses; and even where chromophore absorption overlapped with **AK** (e.g. fluorescein), the sensitisation was clear from the different PSS %*E* reached and the much smaller half-powers required to reach these PSSs (**Fl-AK** vs **AK**; **Figure 3d**; **Supporting Table S5**).

2.5 Mechanistic hypothesis for general assisted switched

So far, the mechanism driving dyad isomerisation was unknown. We excluded intermolecular processes, either between conjugates or involving short-lived intermediates, since the physical mixtures did not show sensitised switching (**Figure 3d** vs **Figure S8**). We had excluded photoredox, not only due to the mismatch of redox potentials, but also since their assisted isomerisation reaches <98%*E* (whereas conjugates whose potentials match for photoredox, all isomerise to >99.7% *E*[24]). Energy transfer from the chromophore to promote an S0→S1 transition of the azobenzene (e.g. FRET) was also excluded since light >700 nm was able to drive the sensitised process rapidly, but this is >250 nm beyond the azobenzene's own absorption i.e. spectral overlap is insufficient (**Supporting Note 4**).

However, azobenzenes' low-lying triplet state, reported at ca. 120-150 kJ/mol[25,26] (equivalent to ca. 800-1000 nm) is energetically accessible; and the observation that all PSSs with significant sensitisation are *E*-enriched, up to but not exceeding 98%, supports populating the azobenzene triplet as it mirrors the ten previously reported intermolecular studies' PSS results (typ. 90-98% *E*)[26,28–32]. We noted that azobenzene has very high spin-orbit coupling coefficients[27,50]; and that it is a remarkably rapid intermolecular quencher of triplet states (~diffusion-limited),[29,31,32] which suggests that a triplet-mediated process might be energetically and kinetically reasonable.

Nevertheless, our observations are incompatible with a normal triplet sensitisation process where triplet energy is transferred to the azobenzene *only after* self-ISC (S1→T1) occurs on the "isolated" chromophore moiety, for several reasons (**Supporting Note 4**). These include, that (i) for self-ISC, the rate of sensitised isomerisation should be proportional to the chromophore's Φ_{ISC}: whereas dyads had nearly identical rates across ≳2 orders of magnitude of Φ_{ISC} (eosin ~ 0.3 vs rhodamine <0.01); and (ii) for self-ISC, the long lifetime of a chromophore triplet ought always to allow it to collide with its azobenzene, such that for a given azobenzene, all chromophores should drive an identical sensitised PSS %*E*: whereas in dyads, substantially different PSSs were seen (e.g. 98%*E* for **NB-AK** but 70-80%*E* with **Cy3**/**Cy5-AK**).

We therefore propose that the mechanism for long wavelength sensitised photoresponse is: (i) excitation of the auxiliary part within the conjugates gives its S1 state with its usual photochemistry (as in the isolated chromophore state); (ii) some fraction of the dyad molecules are *pre-associated:* their azobenzene and chromophore are in close enough molecular contact to form an exciplex; (iii) the exciplex brings the azobenzene's spin-orbit coupling coefficients to bear on the excited state, allowing much more efficient ISC to make an exciplex triplet, than the chromophore could usually perform when isolated; (iv) the exciplex triplet then separates to give the *azobenzene* triplet, which undergoes its usual ultrafast T1→S0 relaxation that can be accompanied by isomerisation favouring an *E*-enriched state (**Figure 4a**). This predicts that the assisted switching efficiency can be much higher than the Φ_{ISC} of the isolated chromophore. (In parallel, the fraction of S1 dyad that is *not pre-associated* undergoes its usual mix of radiative and non-radiative S1→S0 decay, without azobenzene isomerisation.)

It seems reasonable that *E*- and *Z*-isomers of the azobenzene should have different likelihoods of being pre-associated to undergo the exciplex-ISC process, according to the dyad structure. This in turn predicts that the sensitised PSSs of the same azobenzene will differ, depending on the linker and on the chromophore in its dyad. (An extreme case of pre-association being used to tune PSSs was recently published by Klajn, Schapiro *et al.* as "DESC": exploiting *E*/*Z*-dependent triplet sensitisation based on *E*/*Z*-dependent steric fit to achieve up to 95%*Z* long-wavelength sensitised PSS[33], rather than the 98%*E* that would be expected from solution-state sensitisation).

We will propose below that typical pre-associated fractions may be ca. 5-50%, and are up to four-fold larger for the *Z* than the *E* isomer of the same dyad. Since this fraction is relatively high, it will be seen to explain plausibly the two observations that (i) the sensitised process is so photon-efficient that the bulk sensitised photoisomerisation rates are comparable with those for direct azobenzene isomerisation, regardless of whether the chromophore in the dyad has a very low or very high Φ_{ISC}; and relatedly, (ii) at UV wavelengths where the azobenzenes' absorbance is often 2-5 times stronger than that of the chromophore, PSS%*E* values are typically 20-30% higher for conjugates than for the free azobenzenes (see **section 2.6**).

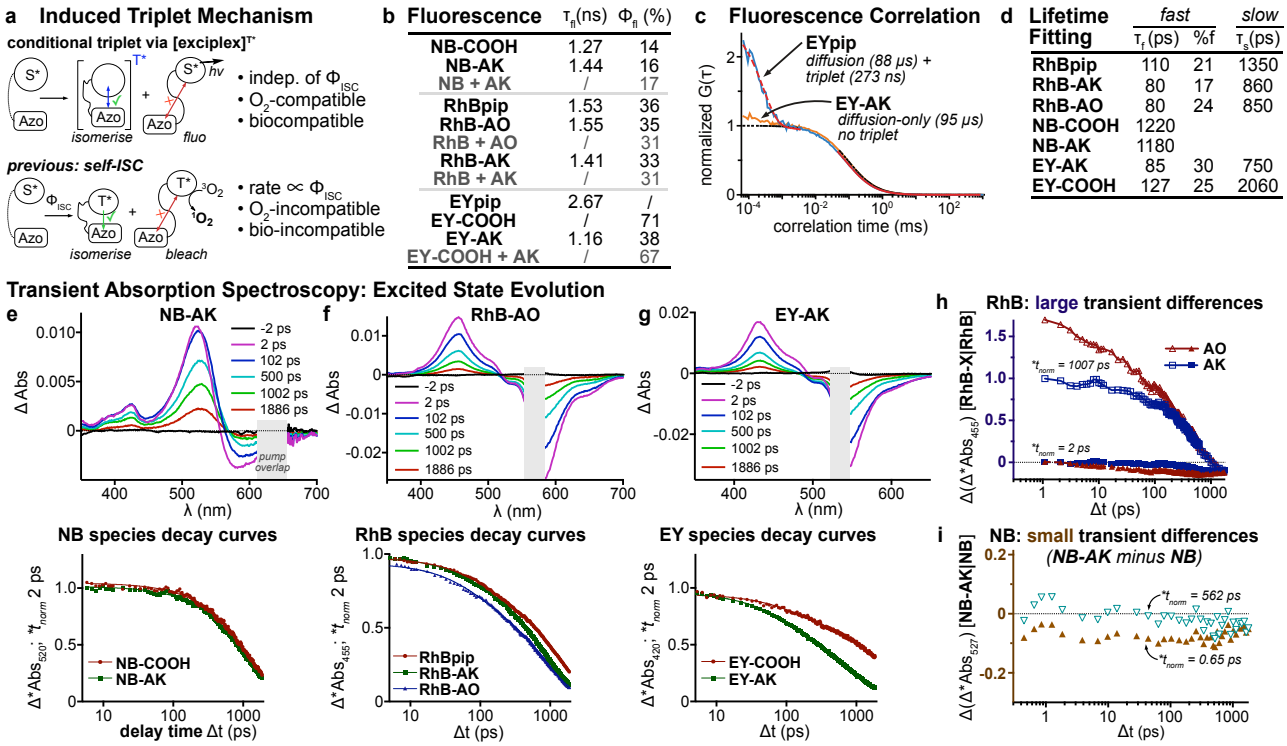

Figure 4: Spectroscopic experiments to study the sensitization-based photoswitching mechanism. **(a)** mechanistic proposal for dyad photoresponse. **(b)** Fluorescence lifetimes and quantum yields for parent chromophores, *E*-dyads, and physical mixtures (grey) ("/" indicates not measured). **(c)** Fluorescence correlation function normalized to the diffusion component (as 1) for eosin (**EYpip**, blue) and eosin-azobenzene dyad (**EY-AK**, orange). The FCS curve for **EYpip** fits a triplet model, but **EY-AK** fits a pure diffusion model (no triplet or other dark states are present). **(d)** Excited state decay kinetics extracted from mono-or biexponential fitted TAS traces. **(e,f,g)** Transient absorption spectra at selected delay times (ΔAbs(Δt,λ)) for **(e) NB-**, **(f) RhB-**, and **(g) EY-** dyads, and excited state decay kinetics of dyads and their parent fluorophores, with "early" (2 ps) normalization. **(h)** Δ(Δ*Abs(Δt,λ)) for (**RhB-AO** minus **RhBpip**) and for (**RhB-AK** minus **RhBpip**), at early (2 ps) and late (1007 ps) normalization. **(i)** Δ(Δ*Abs(Δt,λ)) for (**NB-AO** minus **NB-COOH**) and for (**NB-AK** minus **NB-COOH**), at early (0.65 ps) and late (562 ps) normalization.

It is a crucial feature of the exciplex proposal that the triplet sensitisation in azobenzene dyads does not require prior generation of long-lived triplet states on the *chromophores* (**Figure 4a**). The triplet can be created on the exciplex then collapse to the azobenzene, and these triplets are expected to have ultrashort lifetimes (e.g. azobenzene: picoseconds), quite unlike typical chromophore triplets (microseconds). Therefore, by using chromophores which have tiny Φ_{ISC}, there will be no significant population of triplet states, *except in the exciplexes from pre-associated dyads* which decay rapidly. Thus triplet sensitisation can be achieved without the photochemical drawbacks of long-lived isolated chromophore triplets: making the exciplex triplet process efficient under normal air atmosphere, without singlet oxygen generation, photobleaching, and phototoxicity. Indeed, this is in line with all our experimental observations, where photoswitching was conducted exclusively under air, and without observing photobleaching. This performance is in strong contrast to all previous methods involving azobenzene triplet sensitisation, since in those methods it was assumed that efficient prior generation of a chromophore triplet would be required, but those methods did not allow to quench those triplets quantitatively by the azobenzene. For example, molecular oxygen greatly quenched the triplet-mediated azobenzene isomerisation in solution-state intermolecular triplet sensitisation (isomerisation slows, photobleaching rises); and even with DESC sensitisation, it would be expected that any photosensitiser that is not currently complexed to an azobenzene could be quenched instead by molecular oxygen. Such a predictable "escape" of triplet states with high-Φ_{ISC} dyes would be completely incompatible with biological applications: but in the dyad process with low-Φ_{ISC} dyes, we expected that triplet escape and singlet oxygen generation would not occur since the triplets are only formed *in contact with the azobenzene that is ready to receive and dissipate them fast.*

In case a chromophore itself performs ISC and enters a triplet, this (potentially long-lived) triplet can still perform collisional triplet energy transfer to the azobenzene in its dyad. This "self-ISC" route should be most visible with chromophores that have high Φ_{ISC}, such as eosin **EY** (Φ_{ISC}~0.3): if efficiently quenched by the azobenzene, then its dyads should not have long-lived triplet states (confirmed: **Figure 4c**). However, the exciplex-ISC process does not imply, nor necessarily benefit from, self-ISC running in parallel (see below). Taken together, we simply propose that chromophores do not need a high Φ_{ISC} to drive the exciplex triplet process in azobenzene dyads; but if their Φ_{ISC} is high, then the self-ISC dyads *can* escape the negative photochemistries associated with triplet states, as long as the energy match is reasonable and the linker/attachment design allows the azobenzene to collide more efficiently with the chromophore than e.g. O_2 or other environmental triplet quenchers.

2.6 Mechanistic analysis

We now studied the dyads to test this proposed mechanism: using fluorescence lifetime (τ_{fl}) and fluorescence quantum yield (Φ_{fl}) of the *E*-dyads; fluorescence correlation spectroscopy (FCS) and transient absorption spectroscopy (TAS) of the mostly-*E* dyads (TET-sensitised stationary states, often ca. 6:1 *E*:*Z*); and relative fluorescence intensities of the *E* vs *Z* isomers from fluorimetry during bulk isomerisation. We do not consider these studies mechanistically conclusive, so we only highlight some of the coherent mechanistic aspects, with a full presentation of the data in the **Supporting Information** (Chapters 6-9, **Tables S13-S14, Figures S18-S23**).

(1) We proposed that typically 10% of the *E*-dyads are pre-associated and undergo the exciplex triplet mechanism (we bundle pre-association and exciplex ISC together in the quantum yield $\varphi_{exciplex,E}$). This is not easy to prove, since most measurements (TAS, τ_{fl}, Φ_{fl}) are at best accurate to ±15%. However, for low-Φ_{ISC} chromophores **RhB** and **NB**, τ_{fl} and Φ_{fl} of the *E*-dyads are indeed within measurement error of their isolated chromophores (**Figure 4b**), coherent with ≲15% of their singlet excited states funneling to isomerisation. Dyad Φ_{fl} were strongly *E/Z*-dependent however, with ratios of $\Phi_{fl,E}/\Phi_{fl,Z}$ up to 3.8 for **RhB-AO** (1.9 for **RhB-AK**, etc: **Figure S22-S23**), indicating much more depletion of chromophore S1 states in *Z*-dyads: thus we assume their $\varphi_{exciplex,Z}$ values are higher than their $\varphi_{exciplex,E}$ by this factor. With $\varphi_{exciplex,E}$ values ca. 0.1, this gives $\varphi_{exciplex,Z}$(**RhB-AO**) = 0.2, $\varphi_{exciplex,Z}$(**RhB-AK**) = 0.4, which matches the trend in their bulk 595 nm *Z*→*E* isomerisation kinetics (**RhB-AO** ca. twice as photon-efficient as **RhB-AK**, **Table S3**). These *E/Z*-differences of fluorescence are also coherent with **RhB-AO** having a more *E*-rich sensitised PSS than **RhB-AK** (97% vs 89%, **Fig 1**).

(2) It is also coherent that as conjugates' TAS decays became more rapid than their parent fluorophore (increasing chance of harvesting the chromophore's energy to switch on the single-molecule level), their bulk sensitised photoswitching rates also increased. For example, **RhB** dyads bulk isomerise substantially faster than **NB** dyads (e.g. **Table S5**, half-power 0.23 vs 3.7 mJ/mm^2), which suggests that harvesting energy from **RhB** for switching is more likely than from **NB**. Matching this, while no significant differences are seen in the evolution of **NB-AK** vs **NB-COOH** excited state populations by TAS (**Figure 4eh**), the differences between **RhB-AK**/**-AO** vs **RhBpip** are noticeable (**Figure 4fi**). For **EY-AK**, which had even faster bulk photoswitching, the difference of its TAS decay rate compared to **EY-COOH** was even larger (**Figure 4g**).

(3) **EY** is a chromophore that can perform self-ISC (Φ_{ISC} ~0.3). FCS shows a large triplet fraction for **EYpip**, but no triplet fraction in dyad *E*-**EY-AK** even under high-power illumination (**Figure 4cd**, **Figure S19**). We can interpret this as indicating that ~30% of the excitations of **EY** in the *E*-**EY-AK** dyad are transferred as triplet energy onto **AK**, which reaches a plausible triplet-sensitised PSS (88%*E* at 535 nm). We now compare the switching rates of **EY-AK** to chemically similar dyads whose chromophores should undergo only exciplex-ISC (low Φ_{ISC}; **Fl-AK** and **RhB-AK**). The bulk photoswitching rates of these species are within 20% of those of **EY-AK** under UV (*E*→*Z*) or green (*Z*→*E*) light; and the green light PSS with **RhB-AK** (89%*E* at 564 nm) is also similar to that for **EY-AK** (**Table S5**). This is plausible if $\varphi_{exciplex}$ for **Fl-AK** and **RhB-AK** are similar to the Φ_{ISC} of **EY**: matching the proposed $\varphi_{exciplex}$ range (ca. 0.05-0.5). The similar speeds confirm that self-ISC is not required for photon-efficient assisted switching, and that the exciplex-ISC route can be an efficient assisted switching mechanism regardless of Φ_{ISC}.

(4) We understood these sensitised effects on photoswitching and triplet state depletion are caused by proximity of the switch and fluorophore. We next tested if these behaviours of high-Φ_{ISC} and low-Φ_{ISC} chromophores in dyads, are reproduced by *noncovalently* associating them to azobenzenes. For this we assembled 100% alkylazobenzene lipid vesicles, doped them with 1 mol% of lipidated high-Φ_{ISC} methylene blue (**MB**, $\Phi_{ISC,\ 630\ nm}$: ~0.5) or low-Φ_{ISC} **NB**, and studied the photoswitching of the azo-lipid as well as the chromophores' photostability. Mirroring the results for dyads **EY-AK** vs **RhB-AK**, (i) lipidated high-Φ_{ISC} **MB** drove effective photocatalytic 630 nm *Z*→*E* isomerisation of the azolipid vesicles (**Figure S12b**), but (ii) lipidated low-Φ_{ISC} **NB** was *similarly* photon-efficient in its 630 nm sensitisation of *Z*→*E* vesicle isomerisation as high-Φ_{ISC} **MB** lipid (**Figure S12d**); (iii) lipidated **MB** was entirely photostabilised by the azolipid (quenching of self-ISC triplets which otherwise cause its photobleaching, **Figure S12a**; predictably, **NB** did not photobleach either with or without azolipid: **Figure S12c**). Taken together, this supports that low-Φ_{ISC} chromophores can drive highly photon-efficient assisted switching, without requiring direct triplet generation on the chromophore to initiate it (**Supporting Note 9**).

(5) We also attempted to use the dyads' higher %*E* fraction at UV PSSs, compared to their isolated azobenzenes, to roughly estimate $\varphi_{exciplex}$. Although this involves weak assumptions, it indicated that $\varphi_{exciplex}$ values can be similar to azobenzene $\Phi_{E\rightarrow Z}$ and $\Phi_{Z\rightarrow E}$ values (e.g. for **RhB** conjugates, ca. 0.05 -0.5) which plausibly fits the proposed mechanism (**Supporting Information** section 8.4). We also tried using several modelling techniques to fit the isomerisation *kinetics* as well as the PSS values; but the number of degrees of freedom in these models seems to make data-constrained fitting impossible. We are confident however, that the observed fast isomerisation kinetics and strongly-shifted PSS values indicate that $\varphi_{exciplex}$ can plausibly be on the order of >0.1, even for dyads containing low-Φ_{ISC} chromophores.

By combining this good quantum yield $\varphi_{exciplex}$ with the high long-wavelength extinction coefficients of the chromophores chosen, it seemed that assisted photoswitching could be very photon-efficient. Also, the exciplex proposal does not need to generate damaging chromophore triplets (and the **EY-AK** results show that dyad systems can even *remove* high levels of chromophore triplets generated by self-ISC). Therefore, while the mechanism operating in these dyads remains unclear to us, it seemed that they possessed the right, and unique, combination of photon-efficient unimolecular isomerisation at long wavelengths plus biologically "innocent" photochemistry, that would be needed to apply them in living systems; and we moved forward to testing them in living cells and tissues.

2.7 Sensitiser dyads can harness near-infrared light for biological photocontrol in living cells and acute brain slices

So far, we established that sensitisation by a range of auxiliary chromophores can drive near-complete *Z*→*E* photoisomerization of azobenzenes at 550-770 nm, with high photon efficiency, in biocompatible media, under air, with high photostability: and without re-engineering azobenzene substituents. We next wished to leverage these advances to perform the first single-NIR-photon chemical photoswitching-based control of functions of live cells (**Figure 5**).

NIR-photocontrolling the activity of metabotropic glutamate receptors (mGluRs) is an ideal system that can test all these features while also making excellent use of this performance. mGluRs are G-protein coupled receptors (GPCRs) whose important roles in neuromodulation in the central and peripheral nervous systems make them major drug targets for a range of disorders.[51,52] Due to the importance of discriminating their tissue- and cell-type-specific roles, they have also been a target for photopharmacology for over a decade.[53,54] mGluR2 has seen the most advanced tool development, with photoswitchable glutamates termed “PORTLs” (photoswitchable orthogonal remotely-tethered ligands) that can be covalently tethered with 1:1 stoichiometry onto the receptor via SNAP-tag ligation (**Figure 5a**).[53,55,56] These were chemically refined for higher FDR (more complete photoswitching) as the *para,para'*-anilide/urea "BGAG$_{12,400}$"-type azobenzenes (**Figure 5d**);[49] reworked as branched oligoglutamates that improved the potency of receptor activation;[8] and biological studies have shown how their efficacy translates from cell culture to tissue slice,[53] to acute *in vivo* experiments in freely moving mice, where photocontrol was used to show state-dependent influences of mGluR2 on working memory.[8,49]

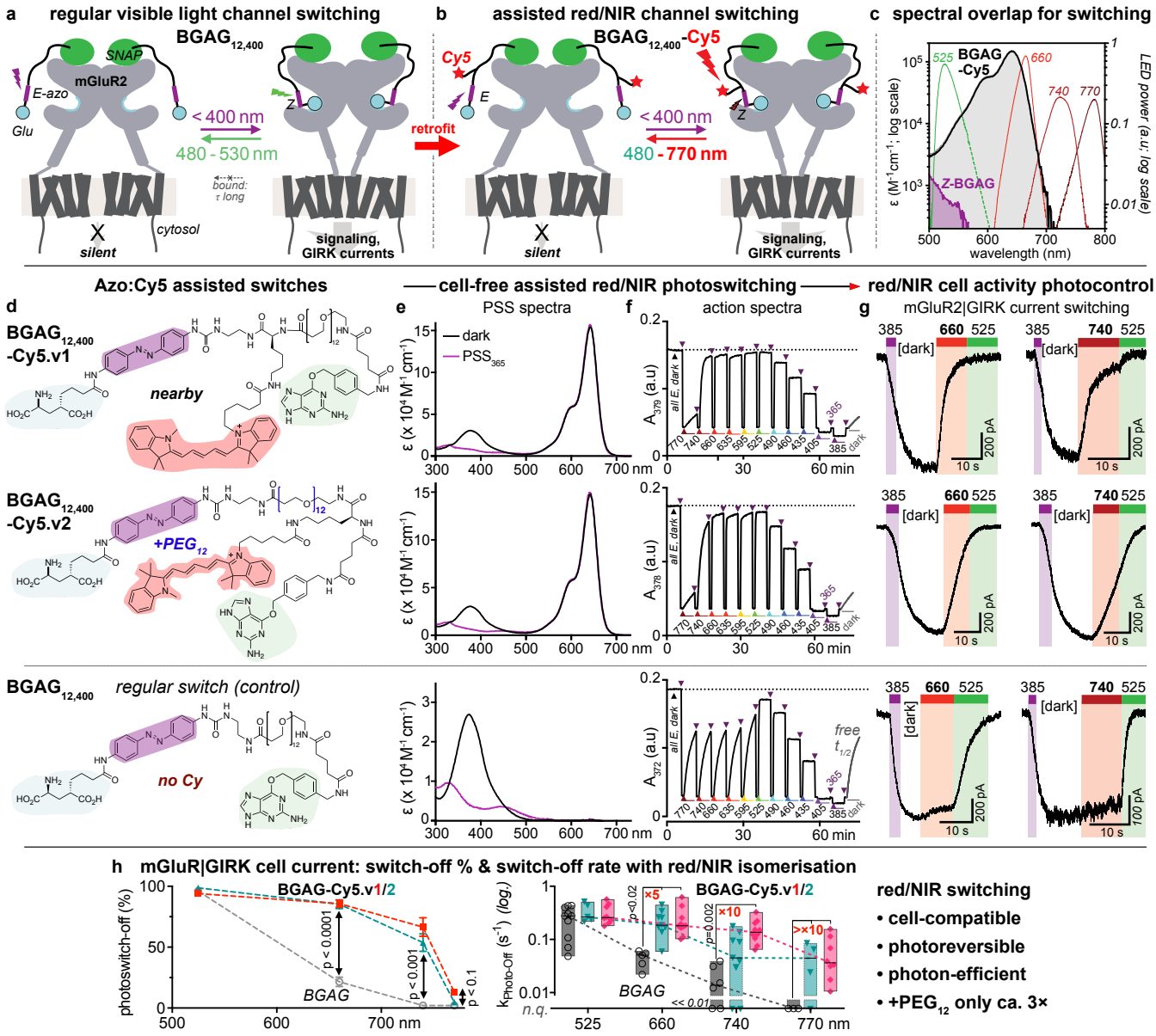

Figure 5: Single-red/NIR-photon photocontrol of GPCR activity in live cells. (**a**) **BGAG$_{12,400}$** is a tethered UV/green-photoswitchable agonist of the SNAP-mGluR2 fusion receptor. (**b-d**) Retrofitting **BGAG$_{12,400}$** with **Cy5** gives **BGAG$_{12,400}$-Cy5s**, primed for operation by LEDs at 660-740 nm. (**e-f**) Cell-free spectra and photoswitching show the unique far-red/NIR photoresponse of **BGAG-Cy5s**; the apparent response of **BGAG$_{12,400}$** in this region is due to its spontaneous relaxation when free (i.e. not receptor-bound; c.f. dark phase relaxation in panel **f**). (**g**) Near-complete *Z*→*E* red/NIR-sensitised "photoswitch-off" of **BGAG$_{12,400}$-Cy5** at 660 nm or 740 nm enables fast, bidirectionally photoreversible switching of mGluR2-evoked GIRK potassium currents in live cells (representative cell current electrophysiology traces in voltage clamp mode during photoswitching). (**h**) Completeness and photon-efficiency rate of mGluR2|GIRK current photoswitch-off (one cell per datapoint, as mean ± SEM; switch-off % at 10 s after start of illumination, with 100% defined as current with all-*E* ligand; **g-h**: HEK293T cells expressing SNAP-mGluR2 and GIRK channels; details in **Figure S24**).

The PORTL tools for ligand:receptor-tethered mGluR2 photopharmacology have powerful performance, particularly as compared to more common photopharmaceutical types e.g. freely-diffusing affinity photoswitches that have usually struggled to reach *in vivo* utility (which we ascribe to the incompleteness and photon-inefficiency of their *Z*→*E* photoswitching, as complicated by biodistribution, *in vivo* inhomogeneity, and light dose limits: **Supporting Note 10**). Nevertheless, we reasoned that by *intrinsically* increasing both the photon efficiency and the completeness of *Z*→*E* photoswitching, while leaving the good performance of the UV *E*→*Z* step untouched, the sensitisation approach might usefully enhance even advanced mGluR2 photopharmaceutical toolsets. Since this ought to be possible without substantially redesigning the photoswitchable ligands, and the red/NIR-light response might even be useful for transcranial photoswitching (fully noninvasive) due to the transparency of biological tissues in the red/NIR, we chose this system for a proof of concept test of whether *in vivo*-capable bidirectional switching could be reached by simple molecular retrofitting. We therefore aimed to test the bidirectionally reversible photoswitchability of mGluR2 currents driven by alternating violet (385 nm) and red/NIR (640-770 nm) illuminations of Cy5-conjugated SNAP-tethered glutamate ligands of type **BGAG$_{12,400}$-Cy5**, compared to their nearly identical congener lacking the cyanine auxiliary, **BGAG$_{12,400}$** (**Figure 5d**).

The conjugates had fast, near-complete red/NIR *Z*→*E* switching in cuvette in physiological media over the whole wavelength range from 595-740 nm (**Figure 5ef**); comparing strongly to the simple ligand **BGAG$_{12,400}$** that is only efficiently switchable ≤525 nm. The isomeric Cy-conjugate **BGAG$_{12,400}$-Cy5.v2**, where the Cy5 motif is

separated from the azobenzene by a PEG_{12} spacer, also reached nearly identical PSSs in cuvette as the proximal **$BGAG_{12,400}$-Cy5.v1**, with only 2.5-fold slower rate for red/NIR-sensitised switching (**Supporting Figure S11**). This was a less severe penalty than we expected for placing the chromophore far from the photoswitch.

We tested these conjugates in HEK293 cells expressing SNAP-mGluR2, which drives G protein-coupled inward rectifier potassium channel (GIRK) currents that allow electrophysiology readouts. Red/NIR-sensitised *Z→E* photoswitching at 660-740 nm controlled GPCR activity, with full photoreversibility when cycled with 385 nm *E→Z* illuminations. As expected from the absorption profile (**Figure 5c**), *Z→E* photoswitching with 660 nm reached near-completion for switch-off of mGluR2 currents more photon-efficiently than 740 nm (**Figure 5gh**): but neither wavelengths switched the simple **$BGAG_{12,400}$**. This provides the first demonstration of nearly *biologically* complete chemical photoswitching-based control of live cell functions using red/NIR light.

Thus, remote functionalisation of a bioactive photoswitch allows it to be operated in sensitised mode, using red/NIR light, to reach excellent efficiency and completion for *in situ Z→E* switching in cell culture. To push towards complex tissue applications, we next investigated whether sensitized switching can also be applied in acute mouse brain slices. For this, we followed a recent protocol[49] injecting Grm2-Cre mice with an adeno-associated virus (AAV) encoding SNAP-mGluR2 allowing the expression of SNAP-mGluR2 in the ventral hippocampus (vHipp). The mice were allowed to express the SNAP-mGluR2 for 2 weeks before locally injecting either **$BGAG_{12,400}$** or **$BGAG_{12,400}$-Cy5-v1** into the vHipp (**Figure 6ab**). After 2 h, acute horizontal slices were prepared, and patch-clamp recordings of granule cells of the dentate gyrus (DG) were performed. As expected, both compounds showed hyperpolarization of the cells following 385 nm induced *E→Z* switching, which was stable when UV light was switched off. Both compounds enabled repolarization of the cells after direct excitation of the azobenzene at 525 nm; but only **$BGAG_{12,400}$-Cy5-v1** also shows repolarization with 660 nm or 740 nm illumination (Cy5-sensitised *Z→E* isomerization; **Figure 6c**), and this red/NIR-based repolarization reaches similar photoswitch-off response as direct 525 nm *Z→E* excitation of the azobenzene in the parent ligand **$BGAG_{12,400}$** (**Figure 6de**). This shows the first ever single-photon far red-operated photoreversible chemical modulation of protein function in acute brain slices.

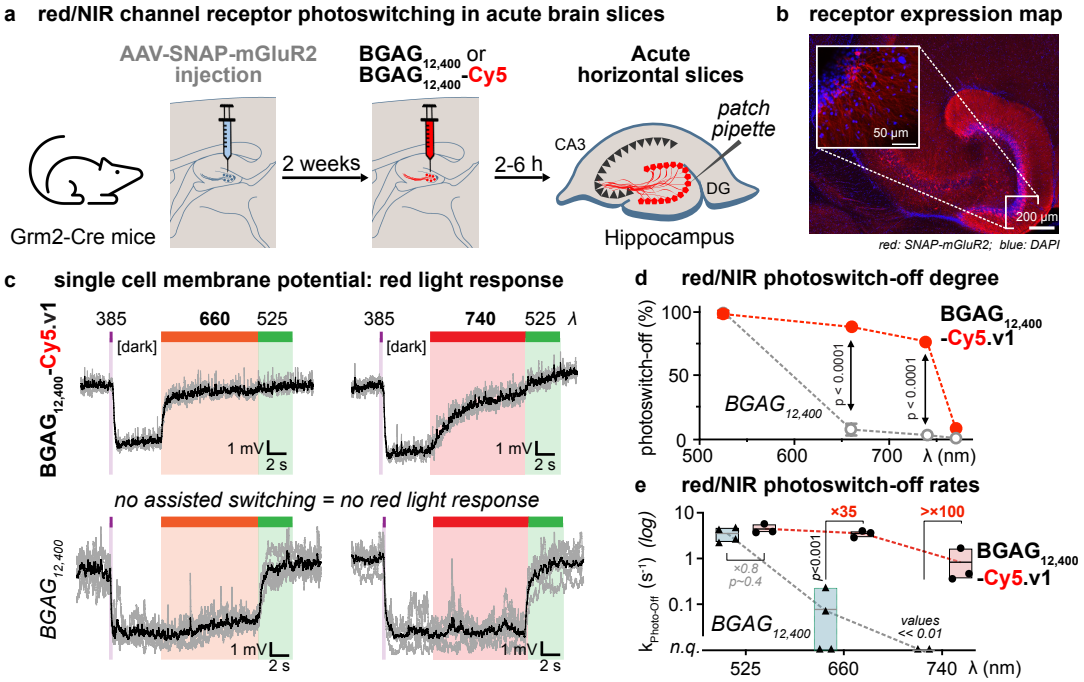

Figure 6: Red/NIR OFF-photoswitching of mGluR2 in intact tissue. (a) Schematic of experimental timeline and configuration of slice recordings. **(b)** SNAP-mGluR2 expression in granule cells of the dentate gyrus as detected by immunohistochemistry (blue: DAPI; red: SNAP-mGluR2). **(c)** Representative whole cell current clamp recordings showing reversible light-induced hyperpolarization/depolarization during five measurement cycles in the same cell (averaged traces in bold). For **$BGAG_{12,400}$-Cy5.v1**, hyperpolarization (385 nm) is reversed by 660 nm or 740 nm illumination, as well as by 525 nm; while for **$BGAG_{12,400}$**, only 525 nm is effective. **(d)** The completeness of "photoswitch-off" (degree of return to 525 nm-equilibrated state, *after* 10 s illumination with the given wavelength) (2-way ANOVA with multiple comparisons). **(e)** The rate of "photoswitch-off": **$BGAG_{12,400}$-Cy5.v1** has significant switchoff rates up to 740 nm; **$BGAG_{12,400}$** does not. *Note the log scale vertical axis with break (n.q.: value <0.01 but not quantifiable).*

3. DISCUSSION AND CONCLUSION

The chromophore-azobenzene dyads reported in this study show a broadly applicable, biocompatible strategy to enable longer-wavelength azobenzene photoisomerisation, and control over downstream biological functions that can be made dependent upon it, than has hitherto been possible. The strategy can be retrofitted onto existing functional photoswitches, with minimal structural changes in the vicinity of the photoswitch itself, and achieves very high-photon-efficiency compared to traditional photoswitch tuning methods The *Z→E* isomerisation following this sensitisation approach can reach 98% red/NIR-completeness with very high efficiency. Although the *Z→E* isomerisation of photoredox dyads, discussed in a parallel paper, is ~100% complete, we feel that the *Z→E* photoisomerisation of these sensitised dyads is not only *better* than any classical azobenzenes, but is also "complete and efficient enough" in an absolute sense: so that now at last, factors other than *Z→E* photoresponse efficiency, wavelengths, and completeness, will become the limiting factors for the performance of azobenzene photoswitches in their intended functional settings.

The two most visible potential drawbacks of this dyad approach are not serious limitations for their performance, in our opinion.

Firstly, the *E*→*Z* isomerisation of the dyads is less complete than the unconjugated azobenzenes, due to competing UV absorption (thus *Z*→*E* sensitisation) by the chromophore. We had chosen **Cy3**, **NB**, and **RhB** for initial dyad studies with the hope that their absorption minima in the near-UV region (**Figure 1c**) could be used as wavelengths for nearly-selective azobenzene excitation, so approaching the typical *E*→*Z* photoswitching completion that azobenzenes are known for. This was reasonably successful, with UV/violet *E*→*Z* ca. 80% complete for conjugates, vs ca. 85-95% complete for free switches; chromophores with lower photoresponses in this region should improve on this. However, since "lit-active" photopharmaceuticals are always preferred for biology,[11] such a small decrease in *E*→*Z* completion is unlikely to make a difference to experimental outcomes: for example, with ca. 1 μM of a *Z*-active **AK**-type lipid photopharmaceutical (as **AK** or as dyad **NB-AK**), 0.95 μM *Z* is not likely to give significantly different performance than 0.8 μM *Z* during an "on-switching" phase - it is rather the completion of the "off-switching" phase which will determine the assay power: in this case, 0.2 μM residual *Z* for **AK** at 500 nm, vs just 0.02 μM residual for **NB-AK** at 640 nm: equating to a 4.5-fold functional dynamic range for **AK** versus *40-fold* functional dynamic range for **NB-AK**.

Secondly, the chromophore may bring complications, such as the potential for chemical or metabolic degradation in the target (biological) system, as well as difficulties in synthesis. However, we believe these can both be mitigated by (a) using the repertoire of (often commercial) chromophores that have been widely developed as highly stable, biocompatible fluorophores, and by (b) optimising the *biological E/Z-based photoswitchability of function* with the simplest possible, non-conjugated azobenzenes, then only *afterwards* attaching auxiliary chromophores that deliver satisfactory sensitised photoswitching performance. This is something of a paradigm shift: until now, photopharmaceutical research has tediously interleaved cycles improving the *E/Z* potency differential with cycles of *E*⇄*Z*-photoswitchability improvement; in many cases, making severe trade-offs such as accepting fast-relaxing compounds even where bistable ligands are biologically more appropriate. Even so, it has often failed to cross the barrier of delivering *in situ bidirectionally photoswitchable* tools that conceptually out-perform unidirectionally photoactuated systems such as photocaged ligands. The decoupling of photochemistry and biology that the sensitisation approach provides should immediately ensure that almost any *Z*-active ligand can now be remotely modified to yield a highly-performing reversibly photoswitchable reagent, which can be used as bistable photopharmaceuticals were always intended: for off/on-photoswitching that is efficient and near-complete in both directions. This decoupling should seriously accelerate research in the current specialist groups, while greatly lowering the barriers for other groups to enter the field.

Alternatively, a poorly chosen chromophore may ruin the systemic or intracellular biodistribution of the dyad, as we suffered with undesired mitochondrial localisation;[35] or if a chromophore is linked in a way which blocks target binding, that will also ruin bioactivity[39]: in some systems, it may not be possible to overcome these. However, reagents whose biodistribution is genetically controlled by ligation to bioorthogonal protein tags, such as the SNAP-Tag ligated reagent used here (**Figure 5** and **6**), offer a very attractive method to avoid both risks. Indeed, many other SNAP- or Halo-ligatable photoswitchable reagents have been published,[53] several of them (particularly for HaloTag) with a fluorophore even incorporated in the system - although none had been examined for the sensitised switching, which we expect that they too will be capable of. Several groups already use fluorescently-labelled photoswitchable ligands, for imaging then photocontrol; by making it known that the fluorescence imaging channel can probably be used to *actuate* these ligands, we hope that this work will promote an inventive variety of conjugates that can complement or out-perform and replace known photopharmaceuticals. Sensitised tethered ligands based around HaloTag may be particularly favoured, since the rates of cellular entry and ligation of HaloTag ligands are multipled by up to 10^4 when rhodamine derivatives are present next to the chloroalkane warhead[57]: an ideal site for rhodamine-based auxiliaries, that are effective sensitisers.

The advantages of this photostable exciplex-ISC sensitised system also give hope for its wide adoption, in biology and beyond. By overcoming the problems of concepts such as the intermolecularity of classical self-ISC triplet sensitisation (inefficient and highly concentration- and environment-dependent), with its associated singlet oxygen mediated photobleaching and phototoxicity (also environment-dependent), this conjugation method usefully enhances the performance of the most important classes of photopharmaceutical scaffolds. Chiefly, the photon efficiency and completeness of the sensitised isomerisation repairs the key problems blocking *Z*→*E* photoisomerisation of any *Z*-active photopharmaceuticals in complex systems or *in vivo*. It is crucial to stress that the intramolecular sensitisation is an *intrinsic* property of the dyads: its operation is independent of concentration, intensity, and assay geometry, so it can be applied in a diversity of settings. These range from sparsely decorated cell-surface receptors in **Figure 5** and **6**, through to moderate concentrations as in the batch switching studies, and we anticipate also to high concentration settings as in films and materials. By avoiding the geometry-/concentration-dependency of two-component photochemistries,[58] the consistent and predictable behavior of such conjugates will be a great benefit for rational development and applications across many labs and uses.

Other advantages may be more relevant to specialised purposes. (1) Simply enabling NIR photocontrol in biology has often been considered a desirable[14,15] although as-yet unreached goal. Our approach now makes that performance available in easily-applicable single-photon mode, at least in the *Z*→*E* direction. We imagine that the challenge of sensitising also the single-photon *E*→*Z* switching process, so that it occurs at distinct but also well-penetrating wavelengths, to allow noninvasive bidirectional photoswitching very deep in tissue or complex media, will attract significant attention. We hope that these hitherto unsuspected opportunities for biocompatible, effective, sensitised photoswitching, which to a degree have been hiding in plain sight, will give that research a significant boost. (2) The self-reporting nature of the photoswitch conjugates can have additional benefits for assessing when sufficient ligand has penetrated to or remains in a target area. (3) Conceptually, this method will also expand possibilities for multi-state addressing of multiplexed photoswitches: e.g., a mixture of (**AK**, **AK-RhB**, **AK-Cy5**) may be set to (*ZZZ*) with 360 nm, (*ZZE*) with 360 then 740 nm, (*ZEE*) with 360 then 595 nm, reset to (*EEE*) with 525 nm, etc; and it should be possible to add further components with spectrally distinct chromophores. On that note, while we did not see any limits on the scope of chromophores that can be used for intramolecular triplet sensitisation, the success of the Cy3 and Cy5 scaffolds in our work directs attention to (i) long-wavelength congeners such as Cy7/Cy7.5/ICG, that have nearly identical bio-relevant properties such as logD, solubility, redox potentials, and biolocalisation, so should operate similarly on cell-surface-labelled receptors; (ii) analogues with different compartmentalisation (e.g. DiI / DiR lipophilic cyanines for lipid environment sensitisation or in-liposome

isomerisation); (iii) new polymethines such as Sletten's MeOFlav7 and JuloFlav7[59,60] which can be excited in the SWIR above 1000 nm; as well as to the increasing range of NIR / SWIR rhodamines[61,62]. It should be noted that the fluorescence brightness of these chromophores should not directly impact their performance as auxiliaries.

In conclusion, we have developed a broadly-applicable, photon-efficient method to perform near-complete *Z*→*E* photoisomerization of a range of azobenzene photoswitches at wavelengths up to the well-penetrating near-infrared region. This method operates within triplet photochemical manifold but is biocompatible, O_2-tolerant, and photostable. No specific re-engineering of azobenzene substituents is needed, so bioactivity or materials properties can be conserved. The auxiliary chromophore of choice can simply be covalently attached in the vicinity of the photoswitch; even when separated by a very long spacer, the sensitised photoresponse can be surprisingly fast, and distance does not compromise the completion it reaches. The quantum yield of the sensitised process can be comparable to that for direct azobenzene *Z*⟷*E* isomerisations, but the far greater extinction coefficients possible for the sensitised *Z*→*E* process allowed our dyads already to reach >50-fold higher photon-efficiency, and at long wavelengths, than optimal direct *blue*-light azobenzene *Z*→*E* switching. We achieve the first ever instance of single-NIR-photon photoswitching of biological activity in acute (live) tissue slices, by actuating metabotropic glutamate receptors labelled with an auxiliary-bearing photoswitchable ligand, whose receptor-binding-photoswitch moiety is otherwise identical to ligands that have been known and painstakingly engineered to deliver multiple cycles of gains in photoresponse over the course of a decade. The straightforward route we now present to overcome the challenges of the *Z*→*E* isomerisation direction, at drastically altered photoresponse wavelengths that can be rationally chosen independently of the photoswitch chemistry, should drive significant progress and innovation in using photoswitches across their full spectrum of applications, from single molecules and logic systems, to bulk materials, and to biology.

ASSOCIATED CONTENT

Supporting Information

PDF containing **Supporting Notes 1-10**, synthetic protocols, NMR spectra, photocharacterisation, analysis and discussion, and biology.
Datafile (XLSX) with *E*/*Z* and PSS spectra of selected compounds.

KEYWORDS: Azobenzene, photoswitch, isomerization, triplet energy transfer, photopharmacology, photochemistry, NIR, photocontrol, molecular switch, exciplex.

AUTHOR INFORMATION

Corresponding Author

Oliver Thorn-Seshold – Department of Pharmacy, Ludwig-Maximilians University Munich, D-81377 Munich, Germany
Email: oliver.thorn-seshold@cup.lmu.de

Author Contributions

BB designed targets, performed synthesis, assembled UV/Vis setup, performed UV/Vis and fluorescence spectroscopy, HPLC analysis, analyzed and coordinated data, assembled figures and contributed to manuscript preparation. VG and FS performed fluorescence lifetime experiments. VG performed fluorescence correlation spectroscopy. AJGH, HM and IA performed cell culture and brain slice experiments. AV performed transient absorption spectroscopy and fluorescence quantum yield measurements. LF designed and wrote the python scripts for mechanism modeling. AMD and MR performed synthesis and photocharacterization. RM and CG performed electrochemical measurements. AO supervised electrochemical measurements. JEB supervised molecular modeling. BDI analyzed and supervised transient absorption spectroscopy and fluorescence quantum yield measurements. JB synthesized $BGAG_{12,400}$-Cy5.v1/2. PT supervised fluorescence lifetime experiments and fluorescence correlation spectroscopy. JL analyzed and supervised cell culture and brain slice experiments. OTS conceived the study, performed synthesis, UV/Vis, data analysis, supervised all other experiments, and wrote the manuscript with input from all authors.

Author Affiliations

(1) Department of Pharmacy, Ludwig-Maximilians University of Munich, D-81377 Munich, Germany; (2) Department of Chemistry, Ludwig-Maximilians University of Munich, D-81377 Munich, Germany; (3) Center for NanoScience, Ludwig-Maximilians University of Munich, D-81377 Munich, Germany; (4) Department of Biochemistry, Weill Cornell Medicine, New York, NY 10065, USA; (5) Leibniz Institute for Photonic Technology Jena e.V. (Leibniz-IPHT), Research Department Functional Interfaces, D-07745 Jena, Germany; (6) School of Chemistry, The University of New South Wales, NSW-2052 Sydney, Australia; (7) Chair for Photonics and Optoelectronics, Nano-Institute Munich, Department of Physics, Ludwig-Maximilians University of Munich, D-80539 Munich, Germany; (8) Institute for Physical Chemistry (IPC), Friedrich Schiller University Jena, D-07743 Jena, Germany; (9) Leibniz Institute for Molecular Pharmacology, D-13125 Berlin, Germany.

Funding Sources

This research was supported by funds from the German Research Foundation (DFG: SPP 1926 project number 426018126 to OTS; SFB1032 Nanoagents for Spatiotemporal Control number 201269156 project B09 to OTS and project A13 to PT and project A08 to TL; Emmy Noether grant TH2231/1-1 number 400324123 to OTS; SFB TRR 152 project P24 number 239283807 to OTS); the National Institutes of Health (R01NS129904 to JL); a Rohr Family Research Scholar Award (to JL); a Monique Weill-Caulier Award (to JL); the Australian Research Council (DP220101847 to JEB); and the Munich Center for Nanoscience (CeNS: to OTS).

ACKNOWLEDGMENTS

BB thanks the Boehringer Ingelheim Fonds for a PhD fellowship. We thank Andrea Stegner and Katja Fußer (LMU) for synthetic support, and Yves Carstensen (FSU) for quantum yield measurements. We are grateful for many insightful and constructive discussions during the ten years of preparation of this paper; in particular we wish to thank Stefan Hecht, as well as Achim Hartschuh, Dirk Trauner, Guglielmo Lanzani, Bert Nickel, Matthew Fuchter, Eberhard Riedle, Thomas Nauser, the attendees of the international Photopharmacology conferences from 2017-2021, and numerous other colleagues, for their insights, encouragement and support.

ABBREVIATIONS

Cy5: cyanine 5; EY: Eosin Y; Fc: ferrocene; FDR: functional dynamic range; Fl: fluorescein; MB: methylene blue; NB: nile blue; NIR: near-infrared; pip: piperazinamide; PORTL: photoswitchable orthogonal remotely tethered ligand; PSS: photostationary state; RhB: rhodamine B; SRhB Sulforhodamine B; TAS: transient absorption spectroscopy; τ_{fl}: fluorescence lifetime; Φ_{fl}: fluorescence quantum yield.

REFERENCES

(1) *Molecular Photoswitches: Chemistry, Properties, and Applications*; Pianowski, Z., Ed.; Wiley, 2022. https://doi.org/10.1002/9783527827626.

(2) Merino, E. Synthesis of Azobenzenes: The Coloured Pieces of Molecular Materials. *Chem. Soc. Rev.* **2011**, *40* (7), 3835–3853.

(3) Pernpeintner, C.; Frank, J. A.; Urban, P.; Roeske, C. R.; Pritzl, S. D.; Trauner, D.; Lohmüller, T. Light-Controlled Membrane Mechanics and Shape Transitions of Photoswitchable Lipid Vesicles. *Langmuir* **2017**, *33* (16), 4083–4089. https://doi.org/10.1021/acs.langmuir.7b01020.

(4) Volgraf, M.; Gorostiza, P.; Szobota, S.; Helix, M. R.; Isacoff, E. Y.; Trauner, D. Reversibly Caged Glutamate: A Photochromic Agonist of Ionotropic Glutamate Receptors. *J. Am. Chem. Soc.* **2007**, *129* (2), 260–261. https://doi.org/10.1021/ja067269o.

(5) Müller, M.; Niemeyer, K.; Urban, N.; Ojha, N. K.; Zufall, F.; Leinders-Zufall, T.; Schaefer, M.; Thorn-Seshold, O. BTDAzo: A Photoswitchable TRPC5 Channel Activator**. *Angewandte Chemie International Edition* **2022**, *61* (36), e202201565. https://doi.org/10.1002/anie.202201565.

(6) Borowiak, M.; Nahaboo, W.; Reynders, M.; Nekolla, K.; Jalinot, P.; Hasserodt, J.; Rehberg, M.; Delattre, M.; Zahler, S.; Vollmar, A.; Trauner, D.; Thorn-Seshold, O. Photoswitchable Inhibitors of Microtubule Dynamics Optically Control Mitosis and Cell Death. *Cell* **2015**, *162* (2), 403–411. https://doi.org/10.1016/j.cell.2015.06.049.

(7) Tsai, Y.-H.; Essig, S.; James, J. R.; Lang, K.; Chin, J. W. Selective, Rapid and Optically Switchable Regulation of Protein Function in Live Mammalian Cells. *Nature Chemistry* **2015**, *7* (7), 554–561. https://doi.org/10.1038/nchem.2253.

(8) Acosta-Ruiz, A.; Gutzeit, V. A.; Skelly, M. J.; Meadows, S.; Lee, J.; Parekh, P.; Orr, A. G.; Liston, C.; Pleil, K. E.; Broichhagen, J.; Levitz, J. Branched Photoswitchable Tethered Ligands Enable Ultra-Efficient Optical Control and Detection of G Protein-Coupled Receptors In Vivo. *Neuron* **2020**, *105* (3), 446-463.e13. https://doi.org/10.1016/j.neuron.2019.10.036.

(9) Laprell, L.; Tochitsky, I.; Kaur, K.; Manookin, M. B.; Stein, M.; Barber, D. M.; Schön, C.; Michalakis, S.; Biel, M.; Kramer, R. H.; Sumser, M. P.; Trauner, D.; Van Gelder, R. N. Photopharmacological Control of Bipolar Cells Restores Visual Function in Blind Mice. *The Journal of Clinical Investigation* **2017**, *127* (7), 2598–2611. https://doi.org/10.1172/JCI92156.

(10) ClinicalTrials.gov. *A Phase I/II Dose-escalating Study of the Safety, Tolerability and Efficacy of Small Molecule KIO-301 Administered Intravitreally to Patients With Retinitis Pigmentosa (ABACUS)*. https://clinicaltrials.gov/study/NCT05282953 (accessed 2023-07-17).

(11) Matsuo, K.; Tamaoki, N. Rational Design and Development of a Lit-Active Photoswitchable Inhibitor Targeting CENP-E. *Org. Biomol. Chem.* **2021**, *19* (32), 6979–6984. https://doi.org/10.1039/D1OB01332G.

(12) Sailer, A.; Meiring, J. C. M.; Heise, C.; Pettersson, L. N.; Akhmanova, A.; Thorn-Seshold, J.; Thorn-Seshold, O. Pyrrole Hemithioindigo Antimitotics with Near-Quantitative Bidirectional Photoswitching Photocontrol Cellular Microtubule Dynamics with Single-Cell Precision. *Angewandte Chemie International Edition* **2021**, *60* (44), 23695–23704. https://doi.org/10.1002/anie.202104794.

(13) Fuchter, M. J. On the Promise of Photopharmacology Using Photoswitches: A Medicinal Chemist's Perspective. *J. Med. Chem.* **2020**, *63* (20), 11436–11447. https://doi.org/10.1021/acs.jmedchem.0c00629.

(14) Hüll, K.; Morstein, J.; Trauner, D. In Vivo Photopharmacology. *Chem. Rev.* **2018**, *118* (21), 10710–10747. https://doi.org/10.1021/acs.chemrev.8b00037.

(15) Velema, W. A.; Szymanski, W.; Feringa, B. L. Photopharmacology: Beyond Proof of Principle. *J. Am. Chem. Soc.* **2014**, *136* (6), 2178–2191. https://doi.org/10.1021/ja413063e.

(16) Beharry, A. A.; Woolley, G. A. Azobenzene Photoswitches for Biomolecules. *Chem. Soc. Rev.* **2011**, *40* (8), 4422–4437. https://doi.org/10.1039/C1CS15023E.

(17) Konrad, D. B.; Frank, J. A.; Trauner, D. Synthesis of Redshifted Azobenzene Photoswitches by Late-Stage Functionalization. *Chemistry – A European Journal* **2016**, *22* (13), 4364–4368. https://doi.org/10.1002/chem.201505061.

(18) Dong, M.; Babalhavaeji, A.; Samanta, S.; Beharry, A. A.; Woolley, G. A. Red-Shifting Azobenzene Photoswitches for in Vivo Use. *Acc. Chem. Res.* **2015**, *48* (10), 2662–2670. https://doi.org/10.1021/acs.accounts.5b00270.

(19) Hansen, M. J.; Lerch, M. M.; Szymanski, W.; Feringa, B. L. Direct and Versatile Synthesis of Red-Shifted Azobenzenes. *Angewandte Chemie International Edition* **2016**, *55* (43), 13514–13518. https://doi.org/10.1002/anie.201607529.

(20) Bléger, D.; Schwarz, J.; Brouwer, A. M.; Hecht, S. *O* -Fluoroazobenzenes as Readily Synthesized Photoswitches Offering Nearly Quantitative Two-Way Isomerization with Visible Light. *J. Am. Chem. Soc.* **2012**, *134* (51), 20597–20600. https://doi.org/10.1021/ja310323y.

(21) Müller-Deku, A.; Thorn-Seshold, O. Exhaustive Catalytic Ortho-Alkoxylation of Azobenzenes: Flexible Access to Functionally Diverse Yellow-Light-Responsive Photoswitches. *J. Org. Chem.* **2022**, *87* (24), 16526–16531. https://doi.org/10.1021/acs.joc.2c02214.

(22) Maier, M. S.; Hüll, K.; Reynders, M.; Matsuura, B. S.; Leippe, P.; Ko, T.; Schäffer, L.; Trauner, D. Oxidative Approach Enables Efficient Access to Cyclic Azobenzenes. *J. Am. Chem. Soc.* **2019**, *141* (43), 17295–17304. https://doi.org/10.1021/jacs.9b08794.

(23) Siewertsen, R.; Neumann, H.; Buchheim-Stehn, B.; Herges, R.; Näther, C.; Renth, F.; Temps, F. Highly Efficient Reversible Z–E Photoisomerization of a Bridged Azobenzene with Visible Light through Resolved S1(Nπ*) Absorption Bands. *J. Am. Chem. Soc.* **2009**, *131* (43), 15594–15595. https://doi.org/10.1021/ja906547d.

(24) Baumgartner, B.; Glembockyte, V.; Mayer, R.; Gonzalez-Hernandez, A.; Kindler, R.; Valavalkar, A.; Wiegand, A.; Müller-Deku, A.; Grubert, L.; Steiner, F.; Gross, C.; Reynders, M.; Grenier, V.; Broichhagen, J.; Hecht, S.; Tinnefeld, P.; Ofial, A.; Dietzek-Ivansic, B.; Levitz, J.; Thorn-Seshold, O. Azobenzenes Can Achieve Near-Infrared Photocontrol in Biological Systems, with Quantitative Z→E Photoisomerization, via Singlet Manifold Photoredox. *ChemRxiv* **2023**. https://doi.org/10.26434/chemrxiv-2023-37sv4.

(25) Monti, S.; Dellonte, S.; Bortolus, P. The Lowest Triplet State of Substituted Azobenzenes: An Energy Transfer Investigation. *Journal of Photochemistry* **1983**, *23* (2), 249–256. https://doi.org/10.1016/0047-2670(83)80065-3.

(26) Bortolus, Pietro.; Monti, Sandra. Cis-Trans Photoisomerization of Azobenzene. Solvent and Triplet Donors Effects. *J. Phys. Chem.* **1979**, *83* (6), 648–652. https://doi.org/10.1021/j100469a002.

(27) Cembran, A.; Bernardi, F.; Garavelli, M.; Gagliardi, L.; Orlandi, G. On the Mechanism of the Cis−trans Isomerization in the Lowest Electronic States of Azobenzene: S0, S1, and T1. *J. Am. Chem. Soc.* **2004**, *126* (10), 3234–3243. https://doi.org/10.1021/ja038327y.

(28) Jones, L. B.; Hammond, G. S. Mechanisms of Photochemical Reactions in Solution. XXX.1 Photosensitized Isomerization of Azobenzene. *J. Am. Chem. Soc.* **1965**, *87* (18), 4219–4220. https://doi.org/10.1021/ja01096a059.

(29) Ronayette, J.; Arnaud, R.; Lemaire, J. Isomérisation photosensibilisée par des colorants et photoréduction de l'azobenzène en solution. II. *Can. J. Chem.* **1974**, *52* (10), 1858–1867. https://doi.org/10.1139/v74-265.

(30) Shimomura, M.; Kunitake, T. Fluorescence and Photoisomerization of Azobenzene-Containing Bilayer Membranes. *J. Am. Chem. Soc.* **1987**, *109* (17), 5175–5183. https://doi.org/10.1021/ja00251a022.

(31) Goulet-Hanssens, A.; Rietze, C.; Titov, E.; Abdullahu, L.; Grubert, L.; Saalfrank, P.; Hecht, S. Hole Catalysis as a General Mechanism for Efficient and Wavelength-Independent Z → E Azobenzene Isomerization. *Chem* **2018**, *4* (7), 1740–1755. https://doi.org/10.1016/j.chempr.2018.06.002.

(32) Isokuortti, J.; Kuntze, K.; Virkki, M.; Ahmed, Z.; Vuorimaa-Laukkanen, E.; Filatov, M. A.; Turshatov, A.; Laaksonen, T.; Priimagi, A.; Durandin, N. A. Expanding Excitation Wavelengths for Azobenzene Photoswitching into the Near-Infrared Range via Endothermic Triplet Energy Transfer. *Chem. Sci.* **2021**, *12* (21), 7504–7509. https://doi.org/10.1039/D1SC01717A.

(33) Gemen, J.; Church, J. R.; Ruoko, T.-P.; Durandin, N.; Białek, M. J.; Weißenfels, M.; Feller, M.; Kazes, M.; Odaybat, M.; Borin, V. A.; Kalepu, R.; Diskin-Posner, Y.; Oron, D.; Fuchter, M. J.; Priimagi, A.; Schapiro, I.; Klajn, R. Disequilibrating Azobenzenes by Visible-Light Sensitization under Confinement. *Science* **2023**, *381* (6664), 1357–1363. https://doi.org/10.1126/science.adh9059.

(34) Isokuortti, J.; Griebenow, T.; Glasenapp, J.-S. von; Raeker, T.; Filatov, M. A.; Laaksonen, T.; Herges, R.; Durandin, N. A. Triplet Sensitization Enables Bidirectional Isomerization of Diazocine with 130 Nm Redshift in Excitation Wavelengths. *Chem. Sci.* **2023**, *14* (34), 9161–9166. https://doi.org/10.1039/D3SC02681G.

(35) Thorn-Seshold, O.; Trauner, D.; Borowiak, M.; Hasserodt, J. EP3137554 - Azoaryls as Reversibly Modulatable Tubulin Inhibitors.

(36) Targowski, P.; Ziętek, B.; Bączyński, A. Luminescence Quenching of Rhodamines by Cyclooctatetraene. *Zeitschrift für Naturforschung A* **1987**, *42* (9), 1009–1013. https://doi.org/10.1515/zna-1987-0914.

(37) Urban, P.; Pritzl, S. D.; Konrad, D. B.; Frank, J. A.; Pernpeintner, C.; Roeske, C. R.; Trauner, D.; Lohmüller, T. Light-Controlled Lipid

Interaction and Membrane Organization in Photolipid Bilayer Vesicles. *Langmuir* **2018**, *34* (44), 13368–13374. https://doi.org/10.1021/acs.langmuir.8b03241.
(38) Pritzl, S. D.; Konrad, D. B.; Ober, M. F.; Richter, A. F.; Frank, J. A.; Nickel, B.; Trauner, D.; Lohmüller, T. Optical Membrane Control with Red Light Enabled by Red-Shifted Photolipids. *Langmuir* **2022**, *38* (1), 385–393. https://doi.org/10.1021/acs.langmuir.1c02745.
(39) Reynders, M.; Oliver Thorn-Seshold. PST2. *in preparation*.
(40) Engdahl, A. J.; Torres, E. A.; Lock, S. E.; Engdahl, T. B.; Mertz, P. S.; Streu, C. N. Synthesis, Characterization, and Bioactivity of the Photoisomerizable Tubulin Polymerization Inhibitor Azo-Combretastatin A4. *Org. Lett.* **2015**, *17* (18), 4546–4549. https://doi.org/10.1021/acs.orglett.5b02262.
(41) Sheldon, J. E.; Dcona, M. M.; Lyons, C. E.; Hackett, J. C.; Hartman, M. C. T. Photoswitchable Anticancer Activity via Trans–Cis Isomerization of a Combretastatin A-4 Analog. *Org. Biomol. Chem.* **2015**, *14* (1), 40–49. https://doi.org/10.1039/C5OB02005K.
(42) Banghart, M.; Mourot, A.; Fortin, D.; Yao, J.; Kramer, R.; Trauner, D. Photochromic Blockers of Voltage-Gated Potassium Channels. *Angew. Chem. Int. Ed.* **2009**, *48* (48), 9097–9101. https://doi.org/10.1002/anie.200904504.
(43) Fortin, D. L.; Banghart, M. R.; Dunn, T. W.; Borges, K.; Wagenaar, D. A.; Gaudry, Q.; Karakossian, M. H.; Otis, T. S.; Kristan, W. B.; Trauner, D.; Kramer, R. H. Photochemical Control of Endogenous Ion Channels and Cellular Excitability. *Nature Methods* **2008**, *5* (4), 331–338. https://doi.org/10.1038/nmeth.1187.
(44) Donthamsetti, P. C.; Broichhagen, J.; Vyklicky, V.; Stanley, C.; Fu, Z.; Visel, M.; Levitz, J. L.; Javitch, J. A.; Trauner, D.; Isacoff, E. Y. Genetically Targeted Optical Control of an Endogenous G Protein-Coupled Receptor. *J. Am. Chem. Soc.* **2019**, *141* (29), 11522–11530. https://doi.org/10.1021/jacs.9b02895.
(45) Konrad, D. B.; Savasci, G.; Allmendinger, L.; Trauner, D.; Ochsenfeld, C.; Ali, A. M. Computational Design and Synthesis of a Deeply Red-Shifted and Bistable Azobenzene. *J. Am. Chem. Soc.* **2020**, *142* (14), 6538–6547. https://doi.org/10.1021/jacs.9b10430.
(46) Stadler, E.; Tassoti, S.; Lentes, P.; Herges, R.; Glasnov, T.; Zangger, K.; Gescheidt, G. In Situ Observation of Photoswitching by NMR Spectroscopy: A Photochemical Analogue to the Exchange Spectroscopy Experiment. *Anal. Chem.* **2019**, *91* (17), 11367–11373. https://doi.org/10.1021/acs.analchem.9b02613.
(47) Frank, J. A.; Moroni, M.; Moshourab, R.; Sumser, M.; Lewin, G. R.; Trauner, D. Photoswitchable Fatty Acids Enable Optical Control of TRPV1. *Nat Commun* **2015**, *6* (1), 7118. https://doi.org/10.1038/ncomms8118.
(48) Frank, J. A.; Yushchenko, D. A.; Hodson, D. J.; Lipstein, N.; Nagpal, J.; Rutter, G. A.; Rhee, J.-S.; Gottschalk, A.; Brose, N.; Schultz, C.; Trauner, D. Photoswitchable Diacylglycerols Enable Optical Control of Protein Kinase C. *Nat Chem Biol* **2016**, *12* (9), 755–762. https://doi.org/10.1038/nchembio.2141.
(49) Gutzeit, V. A.; Acosta-Ruiz, A.; Munguba, H.; Häfner, S.; Landra-Willm, A.; Mathes, B.; Mony, J.; Yarotski, D.; Börjesson, K.; Liston, C.; Sandoz, G.; Levitz, J.; Broichhagen, J. A Fine-Tuned Azobenzene for Enhanced Photopharmacology in Vivo. *Cell Chemical Biology* **2021**. https://doi.org/10.1016/j.chembiol.2021.02.020.
(50) Reimann, M.; Teichmann, E.; Hecht, S.; Kaupp, M. Solving the Azobenzene Entropy Puzzle: Direct Evidence for Multi-State Reactivity. *J. Phys. Chem. Lett.* **2022**, *13* (46), 10882–10888. https://doi.org/10.1021/acs.jpclett.2c02838.
(51) Reiner, A.; Levitz, J. Glutamatergic Signaling in the Central Nervous System: Ionotropic and Metabotropic Receptors in Concert. *Neuron* **2018**, *98* (6), 1080–1098. https://doi.org/10.1016/j.neuron.2018.05.018.
(52) Nicoletti, F.; Bockaert, J.; Collingridge, G. L.; Conn, P. J.; Ferraguti, F.; Schoepp, D. D.; Wroblewski, J. T.; Pin, J. P. Metabotropic Glutamate Receptors: From the Workbench to the Bedside. *Neuropharmacology* **2011**, *60* (7), 1017–1041. https://doi.org/10.1016/j.neuropharm.2010.10.022.
(53) Broichhagen, J.; Levitz, J. Advances in Tethered Photopharmacology for Precise Optical Control of Signaling Proteins. *Current Opinion in Pharmacology* **2022**, *63*, 102196. https://doi.org/10.1016/j.coph.2022.102196.
(54) Gómez-Santacana, X.; Panarello, S.; Rovira, X.; Llebaria, A. Photoswitchable Allosteric Modulators for Metabotropic Glutamate Receptors. *Current Opinion in Pharmacology* **2022**, *66*, 102266. https://doi.org/10.1016/j.coph.2022.102266.
(55) Broichhagen, J.; Damijonaitis, A.; Levitz, J.; Sokol, K. R.; Leippe, P.; Konrad, D.; Isacoff, E. Y.; Trauner, D. Orthogonal Optical Control of a G Protein-Coupled Receptor with a SNAP-Tethered Photochromic Ligand. *ACS Cent Sci* **2015**, *1* (7), 383–393. https://doi.org/10.1021/acscentsci.5b00260.
(56) Levitz, J.; Broichhagen, J.; Leippe, P.; Konrad, D.; Trauner, D.; Isacoff, E. Y. Dual Optical Control and Mechanistic Insights into Photoswitchable Group II and III Metabotropic Glutamate Receptors. *Proc. Natl. Acad. Sci. U. S. A.* **2017**, *114* (17), E3546.
(57) Wilhelm, J.; Kühn, S.; Tarnawski, M.; Gotthard, G.; Tünnermann, J.; Tänzer, T.; Karpenko, J.; Mertes, N.; Xue, L.; Uhrig, U.; Reinstein, J.; Hiblot, J.; Johnsson, K. Kinetic and Structural Characterization of the Self-Labeling Protein Tags HaloTag7, SNAP-Tag, and CLIP-Tag. *Biochemistry* **2021**, *60* (33), 2560–2575. https://doi.org/10.1021/acs.biochem.1c00258.
(58) Walden, S. L.; Rodrigues, L. L.; Alves, J.; Blinco, J. P.; Truong, V. X.; Barner-Kowollik, C. Two-Colour Light Activated Covalent Bond Formation. *Nature Communications* **2022**, *13* (1), 2943. https://doi.org/10.1038/s41467-022-30002-6.
(59) Cosco, E. D.; Arús, B. A.; Spearman, A. L.; Atallah, T. L.; Lim, I.; Leland, O. S.; Caram, J. R.; Bischof, T. S.; Bruns, O. T.; Sletten, E. M. Bright Chromenylium Polymethine Dyes Enable Fast, Four-Color In Vivo Imaging with Shortwave Infrared Detection. *J. Am. Chem. Soc.* **2021**, *143* (18), 6836–6846. https://doi.org/10.1021/jacs.0c11599.
(60) Cosco, E. D.; Spearman, A. L.; Ramakrishnan, S.; Lingg, J. G. P.; Saccomano, M.; Pengshung, M.; Arús, B. A.; Wong, K. C. Y.; Glasl, S.; Ntziachristos, V.; Warmer, M.; McLaughlin, R. R.; Bruns, O. T.; Sletten, E. M. Shortwave Infrared Polymethine Fluorophores Matched to Excitation Lasers Enable Non-Invasive, Multicolour in Vivo Imaging in Real Time. *Nature Chemistry* **2020**, *12* (12), 1123–1130. https://doi.org/10.1038/s41557-020-00554-5.
(61) Sauer, M.; Nasufovic, V.; Arndt, H.-D.; Vilotijevic, I. Robust Synthesis of NIR-Emissive P-Rhodamine Fluorophores. *Org. Biomol. Chem.* **2020**, *18* (8), 1567–1571. https://doi.org/10.1039/D0OB00189A.
(62) Daly, H. C.; Matikonda, S. S.; Steffens, H. C.; Ruehle, B.; Resch-Genger, U.; Ivanic, J.; Schnermann, M. J. Ketone Incorporation Extends the Emission Properties of the Xanthene Scaffold Beyond 1000 Nm†. *Photochemistry and Photobiology* **2022**, *98* (2), 325–333. https://doi.org/10.1111/php.13544.